

X-ray photon-counting detector based on a micro-channel plate for pulsar navigation

Baomei Chen (陈宝梅)^{1,2*}, Baosheng Zhao (赵宝升)¹, Huijun Hu (胡慧君)^{1,2},
Qirong Yan (鄢秋荣)^{1,2}, and Lizhi Sheng (盛立志)^{1,2}

¹State Key Laboratory of Transient Optics and Photonics, Xi'an Institute of Optics and Precision Mechanics,
Chinese Academy of Sciences, Xi'an 710119, China

²Graduate University of Chinese Academy of Sciences, Beijing 100049, China

*Corresponding author: 04cbm@live.cn

Received December 7, 2010; accepted January 14, 2011; posted online May 12, 2011

The pulse time of arrival (TOA) is a determining parameter for accurate timing and positioning in X-ray pulsar navigation. The pulse TOA can be calculated by comparing the measured arrival time with the predicted arrival time of the X-ray pulse for pulsar. In this study, in order to research the measurement of pulse arrival time, an experimental system is set up. The experimental system comprises a simulator of the X-ray pulsar, an X-ray detector, a time-measurement system, and a data-processing system. An X-ray detector base is proposed on the basis of the micro-channel plate (MCP), which is sensitive to soft X-ray in the 1–10 keV band. The MCP-based detector, the structure and principle of the experimental system, and results of the pulse profile are described in detail. In addition, a discussion of the effects of different X-ray pulse periods and the quantum efficiency of the detector on pulse-profile signal-to-noise ratio (SNR) is presented. Experimental results reveal that the SNR of the measured pulse profile becomes enhanced as the quantum efficiency of the detector increases. The SNR of the pulse profile is higher when the period of the pulse is smaller at the same integral.

OCIS codes: 040.7480, 040.3780, 250.0040, 340.7480, 120.1880.

doi: 10.3788/COL201109.060401.

Modern navigators, at present, rely on artificial systems such as the global positioning system (GPS). There are certain situations, particularly with regard to spacecraft navigation, where these systems do not provide a satisfactory solution. The most obvious situation concerns spacecrafts that must operate at an altitude beyond the range of manmade systems. In addition, a spacecraft on a mission of national importance might require additional resources of navigation information in addition to the existing systems to increase their capacity^[1]. The first millisecond pulsar, called the PSR B1913+14, was discovered in 1982^[2]; this discovery provided a new answer to the problem of spacecraft navigation. Astronomers observe pulsars and identify that the majority of millisecond pulsars, whose periods range between 1.5 and 300 ms, have extremely stable rotational velocity. And they are praised to the best clock in the nature. The feasibility of autonomous navigation based on X-ray pulsars has been proved in 1981^[3]; following this, research endeavors on autonomous navigation for spacecraft increased exponentially. In August 2004, the National Aeronautics and Space Administration (NASA) of USA, the Naval Observatory of USA, and other organizations launched a project for pulsar navigation. The primary intention was to manufacture a detection system based on X-ray pulsar navigation^[4].

The pulse time of arrival (TOA) of the X-ray pulsar is the determining parameter for X-ray pulsar navigation. The pulse TOA can be calculated by comparing the measured arrival time with the expected arrival time based on a timing model of the pulsar that has been developed based on years of observation data obtained through ground-based radio telescopes. This pulse TOA can be

translated directly into a correction in the position of the detector in the direction of the pulsar that is under observation. Therefore, the pulse TOA's accuracy determines the accuracy of the positioning and timing for the spacecraft. Thus, a critical aspect of the technique for X-ray pulsar navigation is to develop an X-ray detector which possesses low power, low background and is capable of sub-microsecond timing accuracy on each X-ray photon received^[5]. The micro-channel plate (MCP) X-ray detector has advantages of a long-term working capacity, high detection sensitivity, high signal-to-noise ratio (SNR), wide dynamic range, and high temporal resolution^[6] in comparison with the solid-state semiconductor, gas proportional counter, scintillator, and calorimeter X-ray detectors.

In this letter, we report an X-ray detector based on the MCP, time-measurement system, and data-processing system. The observed pulse profile is fitted after being integrated for 250 s. It can be used for TOA measurement in accordance with the navigation algorithm verification.

Figure 1 presents a schematic diagram of the MCP X-ray detector, which consists of an entrance window, a photocathode, two MCPs, and an anode. The X-ray photons generated from pulsars are in the energy band of 1–10 keV and the pulse flux is extremely faint ($\sim 10^{-5}$ photons/(cm²·s)). Therefore, a 1- μ m-thick polyimide film is used as the entrance window. The transmission of the polyimide film could exceed 75% in the 1–10 keV band^[7]. However, the transmission of 200-eV photons could almost reach 40%. In order to impede photons with energy less than 1 keV, a 50-nm aluminum (Al) film is deposited on the 1- μ m-thick polyimide film. The

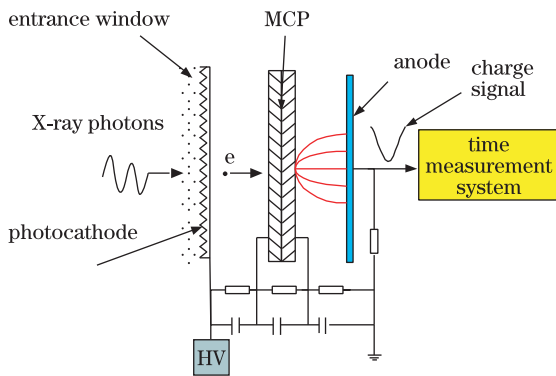


Fig. 1. Schematic diagram of the MCP X-ray detector. HV: high voltage.

transmission of 200-eV photons is thus less than 20%, and the transmission of 1–10 keV photons approximates to 100%^[8]. A 1- μm -thick polyimide film, on which a 50-nm aluminum film has been deposited, constitutes the entrance window which allows sufficient transmission in the 1–10 keV band and restricts transmission at levels less than the 1-keV band.

The basic measurement that yields position and time information is the arrival time of a pulse from the pulsar at the detector. Therefore, one of the key technologies in pulsar navigation is to obtain a high SNR pulse profile. This requires a detector that has a high SNR. Therefore, the detector on the spacecraft should possess high quantum efficiency. The detection quantum efficiency is 5%–10% in the soft X-ray band when X-ray photons directly hit the MCP channel surface^[9]. For this reason, a photocathode with high quantum efficiency in the soft X-ray band is necessary. The quantum efficiency of cesium iodide (CsI) is higher than 1, which is much higher than that of the bare MCP. A comparison of quantum efficiencies of CsI (both planar and deposited on MCP) and gold photocathode indicates that the quantum efficiency of planar CsI is superior^[10]. Therefore, the planar CsI is used as the photocathode in this system.

The MCP is an array of 10^4 – 10^7 miniature electron multipliers that are oriented parallel to each other. The channel matrix is fabricated from lead glass. This type of treatment is undertaken to optimize the secondary emission characteristics of each channel. The saturation gain of channel multipliers is a function of channel length l and the channel diameter d , $\alpha = l/d$. The highest gain originates in the range of the α value from 40:1 to 80:1^[11]. In addition, the quantum efficiency is a function of the MCP input surface angle θ . The peak quantum efficiency occurs in the 1° – 6° range. In this study, in consideration of the difficulty associated with production, two MCPs whose channel diameters were 25 μm with an α value of 40:1 were chosen. Further, both MCPs were arranged in a chevron configuration. This form of arrangement can acquire high electron gain while restraining the ion feedback^[12]. In this detector, the saturation gain of two MCPs exceeds 5×10^7 , and the background count rate is less than 1 photon/($\text{cm}^2 \cdot \text{s}$). The electron-transition time of two MCPs is approximately 1 ns and the electron-transition time distribution is across several hundred picoseconds. This demonstrates that the fast response

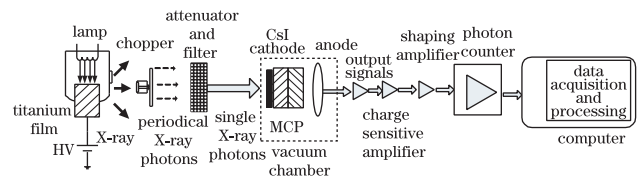


Fig. 2. Schematic diagram of a single photon-counting detection system based on MCP for X-ray pulsar navigation.

and high temporal resolution of this system satisfy the requirements of X-ray pulsar navigation.

The anode is an electron collector behind the MCPs. Thus far, the anode has only been employed for the purpose of timing the pulse. The anode is a copper plate. An accelerating electric field is added in-between the MCP and the anode to collect the output charge cloud from the MCP.

In the experiment, the detector was placed in the vacuum chamber (pressure: $P < 1.3 \times 10^{-4}$ Pa). With the detector working at photon counting module, photons enter the entrance window, hit the photocathode, and are transformed into electrons; these electrons are multiplied by MCPs to form a set of charge clouds. Following the acceleration by an acceleration electric field, these charge clouds are collected by the anode.

The detection system for pulse TOA is a part of the X-ray pulsar navigation system. Thus, an experimental system has been constructed to investigate this critical technological aspect of the detection system. Figure 2 presents a schematic diagram of the experimental system for X-ray pulsar navigation. It comprises of an X-ray tube with titanium target as the X-ray simulator for the X-ray pulsar, a chopper for pulse modulation, an X-ray detector based on MCP in the vacuum system, a time-measurement system, and a data-processing system. The time-measurement system consists of a charge-sensitive preamplifier, a shaping amplifier, and a discriminator. The function of the charge-sensitive preamplifier is to amplify the signal and transform the charge signal into a voltage signal. The shaping amplifier filters the low- and high-frequency noises, and amplifies the input signal. The discriminator functions in the selection of a constant point as the arrival time of the photon event. In the present study, the arrival time of the peak value is used to calculate the arrival time of the photon event. The data-processing system consists of a counter of photon events that is based on a field programmable gate array (FPGA) and a computer with a pulse profile fitting system. Based on the period of the observed pulse, the data-processing system fits the pulse profile by using the data recorded by the counter. The detection system detects the pulse profile of the X-ray pulse. In addition, the measured arrival time can be acquired based on the observed pulse profile. In accordance with the predicted pulse and navigation algorithm, the TOA of the pulse can be calculated.

The time-measurement system is used to mark the arrival time of each detected photon. Therefore, when the input X-ray is sufficiently faint, there is single photon event that is to be detected by the detector; the output signal of the detector is a set of individual random electron pulses. Figure 3(a) depicts the output signal of the

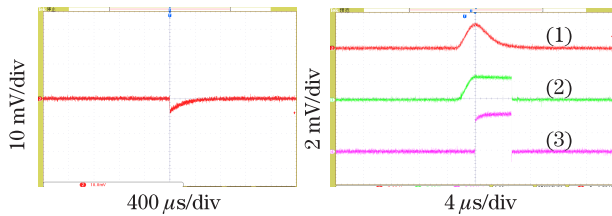


Fig. 3. (a) Detector output signal, (b) time-measurement system output signal.

detector. The signal comprises electrons and, therefore, it is a negative signal. Figure 3(b) shows the output signal of the time-measurement system, which includes the shaping amplifier output and the discriminator output signal. The shaping amplifier output signal is located at the top in Fig. 3(b), the peak hold output signal is in the middle and the trigger output signal is at the bottom. When the peak value of the pulse arrives, the discriminator exports a high level. The experimental conditions for this system include an X-ray tube voltage of 6.5 kV and a current of 70 μ A.

The data-processing system is used to fit the pulse profile. The output signals of the discriminator trigger the photon counter to record the arrival time of the individual photon events. In the course of the total observation, a large number of photons, N , have arrival times ranging from t_0 to t_{N-1} , and these are to be recorded with regard to the system clock. To fit the profile of the pulse, it is necessary to split the recorded time into several periods, and, further, to split a period of the X-ray pulse into several bins during data processing. In addition, the phase of the photon with serial number m can be described as

$$\varphi_m = 2\pi \frac{\text{mod}(t_m, kp)}{p}, \quad m \in [0, N - 1], \quad (1)$$

where φ_m is the phase of the photon whose relative recorded time is t_m , and p is the rotation period of the observed pulsar. The set of photons can be fitted with k periods, where k is an arbitrary integer. A binned pulse profile is reconstructed by dividing the pulse phase into equal bins and dropping each of the N photons into the appropriate phase bin. Then, this set of photons is fitted at the predicted pulse period based on the known timing model of the pulsar. Thus, if this detection system is used in the spacecraft autonomous navigation, there are certain factors that need to be considered, such as the time conversion in different coordinate systems, the Doppler shift, and the effects on time by a clock in motion and with a gravitational potential field^[13].

The fundamental measurement of a pulsar-based navigation system is the pulse arrival time. Further, the accuracy of such a system is determined by the SNR of the profile. The SNR can be described as^[14]

$$\begin{aligned} \text{SNR} &= \frac{N_{\text{pulsed}}}{\sigma_{\text{noise}}} = \frac{N_{\text{pulsed}}}{\sqrt{(N_B + N_{\text{non-pulsed}}) + N_{\text{pulsed}}}} \\ &= \frac{F_X A p_f t_{\text{obs}}}{\sqrt{[B_X + F_X(1 - p_f)](A t_{\text{obs}} d) + F_X A p_f t_{\text{obs}}}}, \quad (2) \end{aligned}$$

where N_{pulsed} denotes the observed X-ray photon flux, $N_{\text{non-pulsed}}$ is the flux of photons which do not come from

the pulsar pulse, σ_{noise} is the standard deviation of noise, N_B is the X-ray background radiation, F_X is the X-ray photon flux from the pulsar, B_X is the X-ray photon flux from the background, A is the effective detection area of the detector, t_{obs} is the observation time, and the pulsed fraction p_f defines the quantity of the source flux that has been pulsed. The duty cycle of a pulse d is determined by the fraction pulse width W and the pulse period p as

$$d = \frac{W}{p}. \quad (3)$$

For a given observation, the TOA accuracy σ_{TOA} can be determined by^[14]

$$\sigma_{\text{TOA}} = \frac{W}{2\text{SNR}}. \quad (4)$$

Figure 4 shows the profiles of pulses which are fitted by a set of single photons. The integral time is 250 s. Comparing Fig. 4(a) with Fig. 4(b), it can be identified that the profile of the pulse in Fig. 4(b) is better than that in Fig. 4(a). This is because CsI is used as a photocathode, which improves the quantum efficiency in comparison with that of the bare MCP; thus, the SNR is improved. However, the contrast between the two is not obvious. This can be attributed to the fact that the thickness of the CsI film is not optimal. Comparing Fig. 4(c) with Fig. 4(a), it can be seen that the period of the pulse in Fig. 4(c) is longer, and the pulse width is the same as that in Fig. 4(a); therefore, the duty cycle of pulse d decreases. The SNR is lower in Fig. 4(a).

The pulse of the simulation X-ray source is accurately reconstructed. From the figure, it can be concluded that this photon-counting detection system can detect the faint X-ray pulse ($\sim 10^{-2}$ photons/($\text{cm}^2 \cdot \text{s}$)), record the arrival time of the individual X-ray photon pulse accurately, and align the individual photons to a pulse profile. In reconstructing the profile of the pulse,

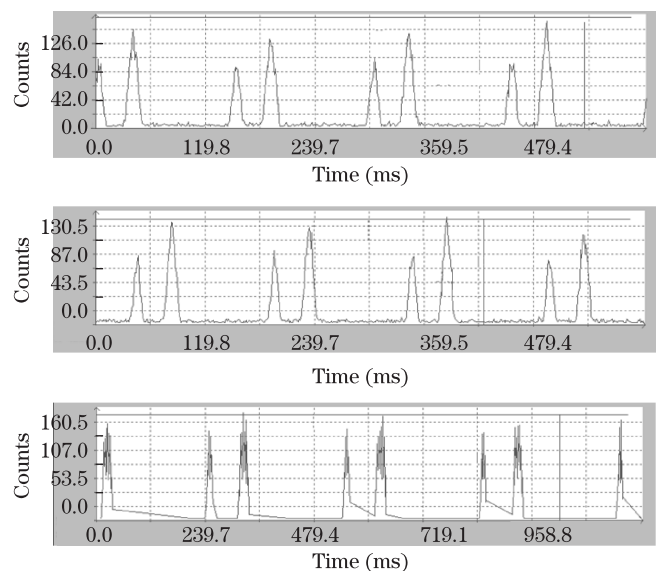


Fig. 4. Profiles of the observed pulses. (a) Four periods with 150-ms period duration based on the bare MCP; (b) four periods using CsI as the photocathode with 150-ms period duration based on the MCP; (c) four periods with 250-ms period duration based on the bare MCP.

the size of bin should be considered to improve the SNR of the pulse profile^[15].

In conclusion, an experimental system, comprising of a simulation X-ray pulsar source, an X-ray detector based on MCP, a time-measurement system, and a data-processing system, is built. Two factors that can affect the SNR of the observed pulse profile — the quantum efficiency of the detector and the duty cycle of a pulse — are discussed. In addition, the temporal resolution and the count rate of the time-measurement system are demonstrated to affect the temporal resolution and the real-time property of the detection system. Therefore, future research should aim to improve the performance of the time-measurement system.

References

1. S. I. Sheikh, D. J. Pines, P. S. Ray, K. S. Wood, M. N. Lovellette, and M. T. Wolff, *J. Guid. Cont. Dyn.* **29**, 49 (2006).
2. L. Nicastro, G. Cusumano, O. Löhmer, M. Kramer, L. Kuiper, W. Hermsen, T. Mineo, and W. Becker, *Astron. Astrophys.* **413**, 1065 (2004).
3. T. J. Chester and S. A. Butman, *NASA Tech. Rep. N81-27129*, 22 (1981).
4. P. Shuai, S. Chen, Y. Wu, C. Zhang, and M. Li, *Chin. J. Space Sci.* (in Chinese) **27**, 169 (2007).
5. F. Zhao, B. Zhao, X. Sai, X. Zhang, Y. Wei, and W. Zou, *Chin. Opt. Lett.* **8**, 361 (2010).
6. M. Gu, D. Wang, C. Ni, X. Liu, S. Huang, and B. Liu, *Acta Opt. Sin.* (in Chinese) **28**, 813 (2008).
7. http://henke.lbl.gov/optical_constants/filter2.html. (December 7, 2010).
8. J. L. Wiza, *Nucl. Instrum. Methods* **162**, 587 (1979).
9. A. S. Tremsin, J. F. Pearson, A. P. Nichols, A. Owens, A. N. Brunton, and G. W. Fraser, *Nucl. Instrum. Methods in Phys. Res. A* **459**, 543 (2001).
10. A. S. Tremsin and O. H. W. Siegmund, *Nucl. Instrum. Methods in Phys. Res. A* **442**, 337 (2000).
11. G. Wang, “Study on 30.4-nm extreme ultraviolet imaging detector” (in Chinese), Master Thesis (Xi’an Institute of Optics and Precision Mechanics, Chinese Academy of Sciences, 2006) pp.20-21.
12. D. F. Ogletree, G. S. Blackman, R. Q. Hwang, U. Starke, G. A. Somorjai, and J. A. Katz, *Rev. Sci. Instrum.* **63**, 104 (1992).
13. J. H. Taylor, Jr., *Proc. IEEE* **79**, 1054 (1991).
14. G. W. Fraser, *X-Ray Detectors in Astronomy* (Cambridge University Press, Cambridge, 1989).
15. H.-J. Hu, B.-S. Zhao, L.-Z. Sheng, and Q.-R. Ran, *Acta Phys. Sin.* (in Chinese) (to be published).